Wave Train Selection Behind Invasion Fronts in Reaction-Diffusion Predator-Prey Models

Sandra M. Merchant *, Wayne Nagata

Institute of Applied Mathematics and Department of Mathematics,

University of British Columbia

Abstract

Wave trains, or periodic travelling waves, can evolve behind invasion fronts in oscillatory reaction-diffusion models for predator-prey systems. Although there is a one-parameter family of possible wave train solutions, in a particular predator invasion a single member of this family is selected. Sherratt (1998) has predicted this wave train selection, using a λ-ω system that is a valid approximation near a supercritical Hopf bifurcation in the corresponding kinetics and when the predator and prey diffusion coefficients are nearly equal. Away from a Hopf bifurcation or if the diffusion coefficients differ somewhat, these predictions lose accuracy. We develop a more general wave train selection prediction for a two-component reaction-diffusion predator-prey system that depends on linearizations at the unstable homogeneous steady states involved in the invasion front. This prediction retains accuracy farther away from a Hopf bifurcation, and can also be applied when predator and prey diffusion coefficients are unequal. We illustrate the selection prediction with its application to three models of predator invasions.

Key words: reaction-diffusion, wave train selection, periodic travelling waves, population cycles, coherent structures, predator invasion

PACS: 87.23.Cc, 05.45.-a

* Corresponding author. Address: Department of Mathematics, Room 121 - 1984 Mathematics Road, The University of British Columbia, Vancouver, B.C., Canada V6T 1Z2. Ph: 1-604-822-9388 Fax: 1-604-822-6074 E-mail: merchant@math.ubc.ca

1 Introduction

The cause of temporal cycles in natural populations has been a focus of study by ecologists for many decades. A classical hypothesis is that this oscillatory behaviour arises from the interaction between a predator population and its prey, and many models have been constructed and studied to support this hypothesis (see, for example [1]). Such models have often taken the form of kinetics systems: ordinary differential equation models that describe the time evolution of predator and prey densities that are assumed to be spatially constant. More recently, however, field studies have shown that in some natural populations oscillations are not synchronized in space, and when viewed in one spatial dimension take the form of a wave train [2–7]. Wave trains, or periodic travelling waves, are spatio-temporal patterns that are periodic in both time and space and have the appearance of a spatially periodic solution that maintains its shape and moves at a constant speed. Consequently, there has been a great deal of study recently on oscillatory reaction-diffusion systems because these partial differential equation models possess wave train solutions (see [8] and references therein).

One way that wave trains can arise in oscillatory reaction-diffusion systems is following a predator invasion [9–11]. The initial condition for such a scenario consists of the prey at carrying capacity everywhere in the spatial domain, except a localized region in which a predator is introduced. Typically, a travelling front evolves that maintains its shape and moves at a constant speed. In some cases, behind this primary invasion front a secondary transition occurs and the solution takes the form of a wave train. Two numerical simulations where wave trains evolve following a predator invasion are illustrated in Fig. 1. We can see from these examples that the wave train behind the front does

not necessarily move at the same speed, or even in the same direction, as the invasion front itself.

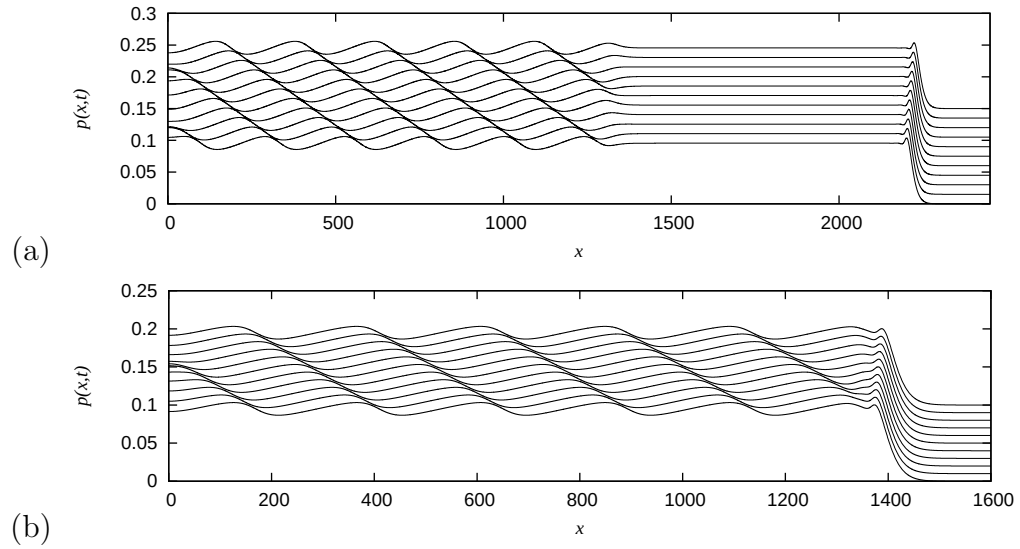

(a)

(b)

Fig. 1. Wave trains behind invasion fronts. The horizontal axis is the spatial coordinate x. Shown are equally spaced plots of the density of the predator $p(x,t)$ at ten equal time intervals with increasing time from bottom to top.

For oscillatory reaction-diffusion systems near a Hopf bifurcation in the corresponding kinetics there exists a one-parameter family of wave train solutions and a range of corresponding speeds [12]. In a particular numerical simulation of an invasion we typically observe only a single member of this family and this seems robust to changes in initial or boundary conditions. Therefore, it appears that a particular wave train is somehow selected out of the family. We would like to find some means of predicting the selected wave train.

Sherratt (1998) has in fact already produced an explanation of the selection mechanism and a prediction for the wave train selected behind invasion fronts in reaction-diffusion systems with oscillatory kinetics [13]. The basis of his prediction is an approximating lambda-omega (λ-ω) system. The behaviour of an oscillatory reaction-diffusion system near a nondegenerate supercritical Hopf bifurcation can be described by the simpler λ-ω system whose coefficients are obtained from the normal form of the Hopf bifurcation in the kinetics sys-

tem. Predictions derived in this way are applicable near the Hopf bifurcation and when the predator and prey have nearly equal diffusion coefficients. For more widely applicable predictions, such as in cases where there are larger amplitude oscillations or unequal diffusion coefficients, it would be beneficial to develop a criterion to predict the selected wave train that does not directly depend on the λ-ω system.

In the remainder of this paper we derive and test such a criterion. We first introduce in section 2 the class of two-component reaction-diffusion systems we consider. These systems describe the evolution of population density distributions of two species, one a prey and the other a predator, in one space dimension. Two spatially homogeneous steady states are relevant: an unstable prey-only state that is invaded by a travelling front, and a coexistence state unstable to oscillatory modes that interacts with the invasion. In some cases, such as illustrated in Fig. 1(a), there is a secondary front that invades the coexistence state. The speed of a front invading an unstable steady state can be predicted by the linear spreading speed (see the review [14] and references therein) which depends only on linearization about the unstable state. In section 3 we consider coherent structures in the complex Ginzburg-Landau (CGL) equation [14–18], of which the λ-ω system is a special case. The unstable state in this case is the origin, which corresponds to the coexistence state in predator-prey systems, and coherent structures represent travelling fronts that connect the steady state to wave trains. The linear spreading speed selects a particular coherent structure and wave train, and this retrieves the prediction developed in [13]. Coherent structures have been generalized as defects in general reaction-diffusion systems by Sandstede and Scheel (2004) in [19]. In section 4 we extend the prediction for the λ-ω system to a new "pacemaker" criterion for defects in predator-prey reaction-diffusion systems that connect

the unstable prey-only state with wave trains associated with oscillatory instabilities of the coexistence state. For the speed of the selected defect we take the minimum of the linear spreading speeds for the prey-only and coexistence states, and for the frequency of the selected wave train measured in the frame comoving with the defect we take the frequency of the linear Hopf instability of the coexistence state. The performance of the pacemaker criterion is then numerically tested in section 5 on sample oscillatory reaction-diffusion systems. We find that the pacemaker criterion gives accurate predictions for a wider range of parameter values than the λ-ω criterion does, but still falls off in accuracy farther away from the Hopf bifurcation. Finally, section 6 discusses and summarizes the key results.

2 Mathematical Background

We consider predator-prey reaction-diffusion systems in one space dimension, of the form

$$\begin{aligned} \frac{\partial h}{\partial t} &= D_h \frac{\partial^2 h}{\partial x^2} + f(h,p) \\ \frac{\partial p}{\partial t} &= D_p \frac{\partial^2 p}{\partial x^2} + g(h,p) \end{aligned} \tag{1}$$

where $h(x,t)$ is the density of prey at position x and time t and $p(x,t)$ is the density of predator at (x,t). Both h and p are real-valued functions. The positive parameters D_h and D_p are the diffusion coefficients of the prey and predator respectively, while the functions $f(h,p)$ and $g(h,p)$ depend on parameters not explicitly shown here, and describe the local population dynamics. For the invasion scenario of interest, we require (1) to have two spatially homogeneous steady states: a prey-only steady state $h(x,t) \equiv 1$, $p(x,t) \equiv 0$ and a coexistence steady state $h(x,t) \equiv h^*$, $p(x,t) \equiv p^*$ where both species persist

at some non-zero levels.

We assume that both the prey-only state $(1, 0)$ and the coexistence state (h^*, p^*) are unstable as fixed points for the corresponding kinetics system

$$\begin{aligned} \tfrac{dh}{dt} &= f(h, p), \\ \tfrac{dp}{dt} &= g(h, p). \end{aligned} \tag{2}$$

In particular we assume that the linearization of (2) about the prey-only state has real eigenvalues of opposite sign, while the linearization about the coexistence state has complex conjugate eigenvalues with positive real part and nonzero imaginary parts, and for some nearby parameter values the coexistence state (h^*, p^*) undergoes a supercritical Hopf bifurcation for (2).

Fig. 1(a) illustrates an invasion that appears to involve two travelling fronts, a primary front invading the unstable prey-only state, and a secondary front invading the unstable coexistence state. The two fronts do not necessarily travel at the same speed. Fig. 1(b) shows there may be a single front invading the prey-only state, but we consider only cases where the dynamics are still influenced by the coexistence state. The speed at which fronts invade an unstable steady state has been the subject of much study. A comprehensive review of this topic is provided by [14]. In this, van Saarloos (2003) defines a linear spreading speed ν^* given by solving the saddle point equations

$$\begin{cases} 0 = S(k^*, \omega^*) \\ 0 = (\partial_k + \nu^* \partial_\omega) S|_{(k^*, \omega^*)} \\ 0 = \Im(\omega^* - \nu^* k^*) \end{cases} \tag{3}$$

for (k^*, ω^*, ν^*) where $S(k, \omega) = 0$ is the characteristic equation for the linearization about the unstable steady state ahead of the front. While there may be multiple solutions to (3), only those for which

$$\Re(D) > 0, \qquad \text{where} \qquad D = \left. \frac{-i(\partial_k + \nu^* \partial_\omega)^2 S}{2\partial_\omega S} \right|_{(k^*, \omega^*)}$$

are relevant. The equivalence of this approach with the historical pinch point analysis is discussed in [20]. When there are several dynamically relevant saddle points we take the one with the largest corresponding ν^* to give the linear spreading speed. Details of how to compute linear spreading speeds using (3) for the system (1) are given in Appendix A. Fronts propagating into unstable states are grouped into two classes: pulled fronts that travel at speed ν^* and are in some sense generic, and pushed fronts that travel at a speed $\nu > \nu^*$. If initial conditions decay sufficiently rapidly in space, faster than $e^{\lambda^* x}$ as $x \to \infty$, where $\lambda^* := \Im(k^*)$, it is argued that a front invading the unstable state forms whose asymptotic speed is ν^* in the case of a pulled front [14]. In this paper, we assume that all fronts we encounter are of the pulled variety, and so travel at the speed given by (3).

Behind the front invading the prey-only state, simulations of predator-prey reaction-diffusion models exhibit a number of different spatio-temporal patterns, including the spatially homogeneous coexistence state, wave trains, and irregular oscillations that have been identified by some as spatio-temporal chaos [9,10,21]. In this paper we restrict our attention to cases where wave trains appear behind the invasion front. The existence of families of wave trains for reaction-diffusion systems has been established by a number of authors [12,22,23]. For solutions that are stationary in a frame moving with speed

$\bar{c}$, (1) may be reduced to the system of ordinary differential equations

$$\begin{aligned}
\tfrac{dh}{d\xi} &= y \\
\tfrac{dp}{d\xi} &= z \\
\tfrac{dy}{d\xi} &= \tfrac{1}{D_h}\left(-\bar{c}y - f(h,p)\right) \\
\tfrac{dz}{d\xi} &= \tfrac{1}{D_p}\left(-\bar{c}z - g(h,p)\right),
\end{aligned} \tag{4}$$

where $\xi = x - \bar{c}t$. It was shown by [12] that if diffusion coefficients D_h and D_p are sufficiently close and the kinetics system (2) has a stable limit cycle near a supercritical Hopf bifurcation, then there exists a one-parameter family of limit cycle solutions for the system (4). This family of limit cycles corresponds to a family of wave train solutions for the reaction-diffusion system (1) near a Hopf bifurcation. In fact, it is known that families of wave trains exist for generic reaction-diffusion systems, for example with unequal diffusion coefficients [23]. We assume that there exists a one-parameter family of wave train solutions for (1).

In many cases, for parameters near the Hopf bifurcation, the rear of the front invading the prey-only state in the reaction-diffusion system (1) remains near the coexistence state for a significant distance before the solution transitions by a secondary front to a wave train, as in Fig. 1(a). In these cases we assume that the speeds of the two fronts are independently determined. Then we focus on the secondary front invading the coexistence state, which connects directly to a wave train. With this motivation, Sherratt (1998) has explained

the selection of a wave train from a one-parameter family in the λ-ω system

$$\begin{aligned} \tfrac{\partial u}{\partial t} &= \tfrac{\partial^2 u}{\partial x^2} + \lambda_0 u - \omega_0 v - (\lambda_1 u + \omega_1 v)(u^2 + v^2) \\ \tfrac{\partial v}{\partial t} &= \tfrac{\partial^2 v}{\partial x^2} + \omega_0 u + \lambda_0 v + (\omega_1 u - \lambda_1 v)(u^2 + v^2) \end{aligned} \tag{5}$$

which can be used to approximate any two-component reaction-diffusion system near a nondegenerate supercritical Hopf bifurcation, provided the diffusion coefficients are equal, or nearly so. Here the real-valued functions $u(x,t)$, $v(x,t)$ represent perturbations from the coexistence state, so the zero state in (5) corresponds to the coexistence state in (1). The constants λ_0, ω_0, λ_1 and ω_1 are the coefficients of the normal form of the Hopf bifurcation in the kinetics system (2), and therefore depend on the parameters of the kinetic terms f and g. In particular, the linearization of the kinetic terms about the zero state has eigenvalues $\lambda_0 \pm i\omega_0$. See [24,25] for more details. We assume in the following that $\lambda_0 > 0$, $\omega_0 > 0$, $\lambda_1 > 0$ and $\omega_1 \neq 0$, thus the zero state is unstable and the Hopf bifurcation in the kinetics system is nondegenerate and supercritical. The advantage of the λ-ω system is that its one-parameter family of wave train solutions can be explicitly written down [12]. These solutions are

$$u(x,t) = r\cos(kx - \Omega t), \qquad v(x,t) = r\sin(kx - \Omega t) \tag{6}$$

where $\Omega = -\omega_0 - \omega_1 r^2$ and $k = \pm\sqrt{\lambda_0 - \lambda_1 r^2}$ are parameterized by the amplitude r. The wave train with amplitude r therefore has phase speed

$$\bar{c} = \frac{\Omega}{k} = \pm\frac{\omega_0 + \omega_1 r^2}{\sqrt{\lambda_0 - \lambda_1 r^2}}. \tag{7}$$

For the λ-ω system (5), Sherratt (1998) predicts that the wave train selected

behind a front invading the zero state is the one with amplitude [13]

$$R = \left[\frac{2\lambda_0}{\omega_1^2} \left(\sqrt{\lambda_1^2 + \omega_1^2} - \lambda_1 \right) \right]^{\frac{1}{2}}. \tag{8}$$

3 Coherent structures and selection in the lambda-omega system

In this section we use the linear spreading speed of a coherent structure in the λ-ω system to find the wave train selected behind an invading front, and thus recover the prediction (8) of [13]. This derivation is implicit in the physics literature cited, but we reproduce it here to motivate the more general selection criterion we use in the case when the λ-ω system is not a good approximation to (1). This derivation also points out that the selected wave train only requires that initial conditions decay sufficiently rapidly in space.

3.1 Coherent structures

The λ-ω system (5) is a special case of the CGL equation, well-studied in the physics literature (see, for example, [15]). We are interested in coherent structures that correspond to travelling fronts connecting a steady state to a wave train.

The one-dimensional (cubic) CGL equation is

$$A_t = \epsilon A + (1 + ic_1)A_{xx} - (1 - ic_3)|A|^2 A, \tag{9}$$

where $A(x,t)$ is a complex-valued function, and ϵ, c_1 and c_3 are real parame-

ters. To write (5) in this form, we put

$$u(x,t) + iv(x,t) = \frac{A(x,t)}{\sqrt{\lambda_1}} e^{i\omega_0 t} \tag{10}$$

in (5) and obtain (9) with

$$\epsilon = \lambda_0, \qquad c_1 = 0, \qquad c_3 = \frac{\omega_1}{\lambda_1}.$$

A coherent structure of the CGL equation (9) is a solution of the form

$$A(x,t) = e^{-i\delta t} a(\xi) e^{i\phi(\xi)}, \qquad \xi = x - \nu t, \tag{11}$$

where a and ϕ are real-valued functions and δ and ν are real parameters. Substituting the ansatz (11) into the CGL equation (9) and defining

$$q = \phi', \qquad \kappa = \frac{a'}{a},$$

we obtain a three-dimensional system of ordinary differential equations for $a(\xi)$, $\kappa(\xi)$ and $q(\xi)$. The existence and linearized stability of fixed points of this three-dimensional system is conveniently summarized in [17, Appendix A]. There are two so-called L (for "linear") fixed points (a_L, κ_L, q_L) with $a_L = 0$, and two N ("nonlinear") fixed points (a_N, κ_N, q_N) with $\kappa_N = 0$. The L fixed points of the three-dimensional system correspond to the homogeneous zero steady state solution for the λ-ω system, while the N fixed points correspond to the wave train solutions (6) of the λ-ω system.

We are interested in heteroclinic orbits of the three-dimensional system, connecting an L fixed point and an N fixed point. These heteroclinic orbits correspond to coherent structures or travelling fronts of the λ-ω system. Due to

symmetry, we consider only the case $\nu > 0$, for a front travelling to the right. Correspondingly, in the three-dimensional system we seek heteroclinic orbits which approach an N fixed point as $\xi \to -\infty$, and approach an L fixed point as $\xi \to +\infty$. If such orbits exist, they must leave along the unstable manifold of the N fixed point and enter along the stable manifold of the L fixed point. Hence, the dimensions of the local stable and unstable manifolds of the L and N fixed points indicate whether the heteroclinic orbits that we seek are at least possible, and whether they can be expected to be robust. Inspecting the eigenvalues of the fixed points reveals that there is an N fixed point with a one-dimensional local unstable manifold, and if $\nu > |\delta|/\sqrt{\lambda_0} > 0$ then there is an L fixed point with a three-dimensional local stable manifold. (If $\delta = 0$ then the three-dimensional system restricted to the invariant plane $a = 0$ is orbitally equivalent to a Hamiltonian system, and in this case there is an L fixed point with a three-dimensional local stable manifold provided $\nu \geq 2\sqrt{\lambda_0}$.) Hence, there is the possibility of a two-parameter family of heteroclinic orbits, parameterized by ν and δ. We have not proved that such a two-parameter family of heteroclinic orbits exists, but for various values of ν and δ we have numerically computed heteroclinic orbits of the three-dimensional system using the continuation software package AUTO and the procedure described in [26–28]. The computations suggest that a two-parameter family of heteroclinic orbits of the three-dimensional system indeed exists.

3.2 Wave train selection

As we have just described, for given coefficients λ_0, ω_0, λ_1 and ω_1 there can be a continuous family of heteroclinic orbits of the three-dimensional system, parameterized by ν and δ. In a particular simulation of the λ-ω system we see

only one of the corresponding front solutions. That is, particular values of ν, δ and the corresponding wave train appear to be selected. Moreover, the selection seems robust to changes in initial conditions and boundary conditions.

We predict the selected front and corresponding wave train in the λ-ω system, by using the linear spreading speed of a pulled front at the zero state $A(x,t) \equiv 0$ of the CGL equation. Application of saddle point equations (3) to the λ-ω system (5) corresponds to selection of the L fixed point with

$$\kappa_L^* = -\sqrt{\lambda_0} \qquad q_L^* = 0,$$

and

$$\nu^* = 2\sqrt{\lambda_0}, \qquad \delta^* = 0 \tag{12}$$

(see [18, pp. 340–341] for details). For the parameter values (12), a heteroclinic orbit connects the selected L fixed point $(0, \kappa_L^*, q_L^*)$ with the corresponding N fixed point $(a_N^*, 0, q_N^*)$, where

$$a_N^* = \sqrt{\lambda_0 - (q_N^*)^2}, \qquad q_N^* = -\frac{\sqrt{\lambda_0}}{\omega_1}\left(\sqrt{\lambda_1^2 + \omega_1^2} - \lambda_1\right). \tag{13}$$

Many authors have observed that fronts in the CGL equation indeed appear to move at the linear spreading speed, but we have no proof that for all initial conditions that decay sufficiently rapidly in space, the selected front must be as predicted, a pulled front moving at the linear spreading speed given by (12). For a few cases, we have compared numerically computed heteroclinic orbits of the reduced system to the front solutions produced by direct simulation of the λ-ω system. In all the cases we studied, we found close agreement between the predicted and observed coherent front solutions. From other simulations we observe that this agreement also appears to be robust with respect to

perturbations of the initial condition.

With the parameters given by (12), the front solution for the λ-ω system (5) is a coherent structure

$$u(x,t) + iv(x,t) = \frac{a(\xi)}{\sqrt{\lambda_1}} e^{i\omega_0 t} e^{i\phi(\xi)}, \qquad \xi = x - \nu^* t,$$

with frequency ω_0 and moving to the right with speed $\nu^* = 2\sqrt{\lambda_0}$. As $\xi \to +\infty$ the front solution approaches the homogeneous zero steady state, and as $\xi \to -\infty$ it approaches the wave train solution

$$u(x,t) + iv(x,t) = \frac{a_N^*}{\sqrt{\lambda_1}} e^{i\omega_0 t} e^{iq_N^* \xi}. \tag{14}$$

To see the relation with the prediction (8) from [13], we note that a wave train solution of the λ-ω system (5) of the form

$$u(x,t) + iv(x,t) = re^{i(kx - \Omega t)}$$

under the change of variables $\xi = x - \nu^* t$ becomes

$$re^{i(\nu^* k - \Omega)t} e^{ik\xi}.$$

Comparing with (14), we see that in the comoving frame the selected wave train has temporal frequency

$$\nu^* k - \Omega = \omega_0 \tag{15}$$

and spatial wavenumber

$$k = q_N^*.$$

Substitution of this wavenumber using (13) to find the amplitude of the selected wave train $r = a_N^*/\sqrt{\lambda_1}$ retrieves the prediction (8) derived by [13]. We have verified this selection with numerical simulations of the λ-ω system using randomly-generated initial conditions. See Fig. 3(i).

We note in (15) that the frequency of the selected wave train in the frame comoving with the selected coherent structure coincides with the imaginary part of the complex eigenvalue $\lambda_0 + i\omega_0$ of the kinetics system for (5) linearized around the unstable zero state. We can therefore think of the linear Hopf frequency ω_0 at the zero state as a "pacemaker", in the sense that the selected wave train in the frame moving with speed $\nu^* = 2\sqrt{\lambda_0}$ must have the same temporal frequency ω_0.

4 Beyond the lambda-omega system: the pacemaker criterion

In this section we consider wave train selection behind invading fronts in the predator-prey reaction-diffusion systems described in section 2. In general for the full oscillatory reaction-diffusion systems (1), wave trains are not sinusoidal and we do not have exact solutions for them, so a prediction of the form (8) is not possible. However, as shown in Fig. 1, numerical simulations of predator invasions in the full system even well away from the Hopf bifurcation in the kinetics still appear to have travelling fronts connecting steady states to wave trains. For the full system we assume there exist two wave train selection regimes, which we refer to here as Case I and Case II.

In Case I, suggested by Fig. 1(a), we assume there is a primary front invading the prey-only state with speed c_{inv} that connects to the coexistence state and that is stationary in the frame comoving with speed c_{inv}, and a secondary

front invading the coexistence state with speed c_{sec} that connects to a wave train and is temporally periodic in the frame comoving with speed c_{sec}. We assume the two fronts can be treated independently, and the relevant front for selection is the secondary one connecting the coexistence state to the wave train. In this case selection is directly analogous to selection in the λ-ω system. In Case II we assume there is a front with speed c_{inv}, temporally periodic in the frame comoving with speed c_{inv}, that connects the prey-only state directly with the selected wave train, as suggested by Fig. 1(b). In addition, we assume that there exists, at least nearby, a front with speed c_{sec} connecting the coexistence state to the wave train. In both cases we assume the fronts are pulled and so the speeds c_{inv} and c_{sec} are the linear spreading speeds obtained by linearization about the spatially homogeneous prey-only and coexistence steady states respectively.

In both Cases I and II, we propose that the speed c_{coh} of the front that selects the wave train is the minimum of the two speeds defined above,

$$c_{coh} := \min\{c_{sec}, c_{inv}\},$$

and we assume the front moves to the right: $c_{coh} > 0$ (for fronts moving to the left, replace x with $-x$). Our justification for this value of the selecting front speed is as follows. First, if $c_{sec} < c_{inv}$ then we predict that the tail of the primary invasion front decays to the coexistence state (h^*, p^*) and behind the primary front a secondary transition occurs from the coexistence state via a front with speed $c_{coh} = c_{sec}$. This corresponds to Case I of the criterion. If, on the other hand $c_{sec} > c_{inv}$, such a secondary front could not exist for long since it would catch up to the primary front. In this case, we therefore predict that eventually the primary invasion front moving with speed $c_{coh} = c_{inv}$ will not

decay to the coexistence steady state and instead connect directly from the prey-only state to the selected wave train, which is Case II. With this picture in mind, we will sometimes refer to Case I as "separated" and to Case II as "attached" to aid in remembering them.

In analogy with the selection criterion (15) for the CGL equation we conjecture that in the comoving frame of speed c_{coh} the selected wave train has the frequency ω_{coh} of the linear unstable oscillatory mode of the coexistence state. To express this selection criterion in terms of the wave train parameters, let $L > 0$ be the spatial period, c_{wtrain} be the phase speed and $T = L/c_{wtrain}$ be the (signed) temporal period of the selected wave train. Then the frequency of the wave train in the comoving frame of speed c_{coh} is $(2\pi/L)c_{coh} - (2\pi/T)$. Our criterion for the selected wave train is that it satisfies

$$\frac{2\pi}{L}c_{coh} - \frac{2\pi}{T} = \omega_{coh} \tag{16}$$

where the "pacemaker" frequency ω_{coh} is the imaginary part of the eigenvalue of the linearization of the kinetics system about the coexistence state:

$$\omega_{coh} = -\mathrm{sgn}(\omega_0\omega_1)\,\frac{1}{2}\sqrt{-\left(\frac{\partial f}{\partial h} - \frac{\partial g}{\partial p}\right)^2 - 4\frac{\partial f}{\partial p}\frac{\partial g}{\partial h}}\Bigg|_{(h^*,p^*).} \tag{17}$$

where ω_0 and ω_1 are two of the normal form coefficients of the Hopf bifurcation in the corresponding kinetic system. We note that since here the selection criterion depends on these kinetic normal form coefficients we are assuming that the system is sufficiently close to a supercritical Hopf bifurcation in the kinetics.

If $f(h,p)$ and $g(h,p)$ are given by the kinetics of the λ-ω system, the selection criterion (16) is the same as the selection criterion (15) using the linear

spreading speed for the λ-ω system, with $\omega_{coh} = \pm\omega_0$, $c_{coh} = 2\sqrt{\lambda_0}$, $L = 2\pi/|k|$ and $T = \pm 2\pi/\Omega$, and so we have in some sense extended the prediction for the λ-ω system to one that may be used on the full system. We acknowledge that in Case II (attached), as in Fig. 1(b), the coexistence state (h^*, p^*) is not approached and so there is no good reason to expect that the pacemaker frequency ω_{coh} plays a role as the frequency in the selection criterion. Nevertheless, it performs surprisingly well as a predictor in numerical simulations and so we continue to use it for the selection criterion.

While the *motivation* for the criterion has a fairly sound mathematical basis, the criterion itself is a somewhat naive extension of those ideas. Essentially, we are assuming that a generalized temporally periodic "coherent front" solution exists that connects a steady state (either prey-only or coexistence) to the selected wave train solution. Furthermore, we are assuming that this coherent front is of the pulled variety and, critically, we are assuming that we know the period $2\pi/\omega_{coh}$ of this coherent front. The criterion (16) therefore has the drawbacks that these assumptions may be false. However, the criterion has a number of advantages. Most obviously, it may be applied to systems other than the λ-ω system. In addition, although the motivation for the criterion depends on the diffusion coefficients of the two species being equal, the criterion itself does not require this.

5 The Criterion in Practice

To study the validity of the criterion (16) we have considered three particular forms for the kinetic equations in the oscillatory reaction-diffusion system (1) as well as a λ-ω system. That is, we consider the four sets of kinetics

$$(i)\ \ f(h,p) = \lambda_0 h - \omega_0 p - (\lambda_1 h + \omega_1 p)(h^2+p^2) \qquad (ii)\ \ f(h,p) = h(1-h) - \frac{hp}{h+C}$$
$$g(h,p) = \omega_0 h + \lambda_0 p + (\omega_1 h - \lambda_1 p)(h^2+p^2) \qquad g(h,p) = -Bp + A\frac{hp}{h+C}$$

$$(iii)\ \ f(h,p) = h(1-h) - p\left(1-e^{-Bh}\right) \qquad (iv)\ \ f(h,p) = h(1-h) - A\frac{hp}{h+C}$$
$$g(h,p) = Cp\left(A-1-Ae^{-Bh}\right) \qquad g(h,p) = Bp\left(1-\frac{p}{h}\right)$$

where ω_0, ω_1, λ_0, λ_1, A, B and C are parameters. Models (ii)-(iv) all assume a logistic growth for the prey species in absence of the predator and assume a saturating functional response for the predation term, but differ in how this saturation and resulting predator growth are modelled [1]. In addition, (ii)-(iv) have all been utilized in the past to model predator invasions and the production of wave trains following the primary invasion front [9,10]. Our goal here is to both illustrate how one would apply the selection criterion (16), as well as to study the accuracy of the criterion for these well-known kinetics and compare with the prediction that would be arrived at using the λ-ω system.

5.1 Equal Diffusion Coefficients

For each model we set $D_h = D_p = 1$ and chose a bifurcation parameter (B for models (ii)-(iv) and λ_0 for model (i)) for which the coexistence steady state in the kinetic system undergoes a supercritical Hopf bifurcation as this parameter is varied. All other parameters of each model were fixed at the values shown in Table 1. For each of models (ii)-(iv) we computed the corresponding normal form parameters for the kinetics, and note that in this normal form the bifurcation parameter B is linearly related to the parameter λ_0 of the λ-ω system kinetics (i) by the relation shown in the final row of Table 1, with the

supercritical Hopf bifurcation occurring at $\lambda_0 = 0$. Also, for computational convenience, the remaining parameters, A and C for (ii)-(iv) and λ_1, ω_0 and ω_1 for (i), were fixed at values that resulted in the same values of the corresponding normal form parameters ω_0 and $c_3 = \omega_1/\lambda_1$. Hence, for a given value of the parameter λ_0, all models have the same predictions for selected speeds of wave trains using the λ-ω system.

Table 1
Parameter Values for Models (i)-(iv)

Model	(i)	(ii)	(iii)	(iv)
A	-	0.15	3.02173	6.92368
C	-	0.2	0.02923	0.63542
ω_0	0.14142	-	-	-
λ_1	9.25926	-	-	-
ω_1	-14.32219	-	-	-
λ_0	-	$8(0.1 - B)$	$0.03684(B - 2.54504)$	$0.02268 - B$

For each of the models (i)-(iv) we computed the predicted selected wave train using (16) by numerical continuation with the software package AUTO. We continued the system (4) in the kinetic bifurcation parameter λ_0 as a boundary value problem with periodic boundary conditions subject to the constraint (16). In tandem with this, we also continue the linear spreading speed equations as outlined in Appendix A for the speeds c_{sec} and c_{inv} that correspond to Cases I (separated) and II (attached) of the criterion respectively. We note that since the secondary front speed goes to zero at the Hopf bifurcation, Case I of the criterion applies near the Hopf bifurcation at $\lambda_0 = 0$ and Case II may apply farther away from the bifurcation point, with the exchange between the two cases occurring if these two curves cross.

We briefly mention here how we determined initial solutions for the contin-

uation of the selection criterion. Two different means were used to find an initial wave train that satisfies (16). Case I (separated) of the criterion always applies close to the Hopf bifurcation in the kinetics and so in this case we start at $\lambda_0 = 0.0001$ and use the analytical criterion (8) from the λ-ω system to find an approximate wave train speed to start. We then continue in the speed parameter the system (4) from the Hopf bifurcation to a wave train of the desired speed. For Case II (attached) of the criterion we started the continuation at $\lambda_0 = 0.005$ and so the λ-ω system may not be a good approximation. In this case, we first generated a series of wave trains of different speeds by continuation in $\bar{c}$ of system (4). For each of these wave trains we computed the temporal frequency $(2\pi/L)c_{inv} - (2\pi/T)$ in the c_{inv} frame and the wave train with temporal frequency nearest to ω_{coh} was used as the starting point for the continuation. The speeds of these predicted wave trains found by continuation are shown as curves in Fig. 3. In this figure solid curves correspond to criterion (18) with $c_{coh} = c_{sec}$, dashed curves use the criterion with $c_{coh} = c_{inv}$ and the criterion with the proposed speed $c_{coh} = min\{c_{sec}, c_{inv}\}$ corresponds to the uppermost of these two curves.

To compare with these predictions, we performed numerical simulations of each system over a range of the bifurcation parameter. Simulations were performed using a finite-difference discretization of the system (forward differences in time and centered differences in space) in the comoving frame of speed $-c_{coh}$ (computed as above) on the interval $[-l, 0]$ with boundary conditions

$$h(-l,t) = 1,\ p(-l,t) = 0 \qquad \frac{\partial h}{\partial \xi}(0,t) = 0,\ \frac{\partial p}{\partial \xi}(0,t) = 0$$

for models (ii)-(iv), and for model (i)

$$h(-l,t)=0, p(-l,t)=0 \qquad \frac{\partial h}{\partial \xi}(0,t)=0, \frac{\partial p}{\partial \xi}(0,t)=0.$$

where $\xi = x + c_{coh}t$. We note that our numerical simulations are of leftward moving fronts for computational convenience and so we perform the coordinate transformation $\xi \mapsto -\xi$ for later comparison with predictions made from the criterion (16). The domain length l was chosen so that the primary invasion front remained far from the left boundary for the duration of the simulation; we set

$$l = \begin{cases} 2000 + T_{end}(c_{inv} - c_{sec}), & c_{sec} < c_{inv} \\ 2000, & c_{sec} \geq c_{inv} \end{cases}$$

where T_{end} is the final time for the numerical simulation. The initial condition used for simulations of models (ii)-(iv) was

$$h(\xi,0) = \begin{cases} h^*, & \xi \geq -1000 \\ 1, & \xi < -1000 \end{cases}, \quad p(\xi,0) = \begin{cases} p^*, & \xi \geq -1000 \\ 0, & \xi < -1000 \end{cases}$$

and for model (i) we initialized the system at the $(h,p) = (0,0)$ state everywhere with the addition of white noise of magnitude $\epsilon = 0.001$ on the subinterval $[-1000, 0]$. Most simulations were run up to a final time $T_{end} = 10000$, with a few cases run to $T_{end} = 20000$ for the model (iv) because the evolution of the selected wave train in these cases was so slow that no wave train was observed at time $t = 10000$. A snapshot of the spatial distribution of the predator and prey populations was saved at times $t = 981, 982, 983, ..., 1000$, $t = 1981, 1982, ..., 2000$ etc. for the computation of the "observed" speed of the wave train selected by the primary front.

Similarly to the reaction-diffusion systems, linear spreading speeds may also be computed for finite difference systems such as our discretization here and in general differ from the continuum system (for example, see [20]). Since the linear spreading speed c_{coh} is a key component of our selection criterion, we chose the spatial mesh size $\Delta\xi$ and the timestep Δt so that the linear spreading speed for the discretized system was within 0.5% of the continuum value. This required different choices for $\Delta\xi$ and Δt in different parameter regions for each of the models, which we summarize Table 2.

Table 2
Mesh Interval and Timestep for Numerical Simulations

		Range in λ_0			
		(i)	(ii)	(iii)	(iv)
$D_h = 1,\ D_p \leq 1$	$\Delta\xi = \frac{1}{4},\ \Delta t = \frac{1}{50}$	[0.02,0.295]	[0.023,0.199]	[0.03,0.195]	[0.014,0.022]
	$\Delta\xi = \frac{1}{8},\ \Delta t = \frac{1}{200}$	[0.005,0.015]	[0.007,0.021]	[0.005,0.025]	[0.007,0.0135]
	$\Delta\xi = \frac{1}{16},\ \Delta t = \frac{1}{800}$	-	[0.003,0.005]	-	[0.002,0.0065]
$D_h = 1,\ D_p = 2$	$\Delta\xi = \frac{1}{4},\ \Delta t = \frac{1}{100}$	-	[0.025,0.195]	[0.03,0.19]	-
	$\Delta\xi = \frac{1}{8},\ \Delta t = \frac{1}{400}$	-	[0.005,0.02]	[0.005,0.01]	-

For each set of parameter values, the spatial profiles were plotted at times $t = 1000, 2000, 3000, ...$ and visually inspected. For the majority of cases, a wave train did appear to evolve behind the primary invasion front and maintained its form over time. For some parameter sets of models (ii) and (iii) in the Case I (separated) parameter region, however, a selected wave train was only observed transiently. In these cases, there does initially appear to be a secondary "front" of speed c_{sec} that selects a wave train, but after some finite time the secondary transition moves faster than the predicted speed c_{sec}, as illustrated in Fig. 2, and the region behind the invasion became irregular for later times.

For the speeds of wave trains in the simulations, the final set of 20 profiles was used to compute this speed if the wave train remained regular throughout the timeseries. If, however, the wave train in the final data set appeared irregular as in Fig. 2, then we instead used the last set of profiles prior to the change in

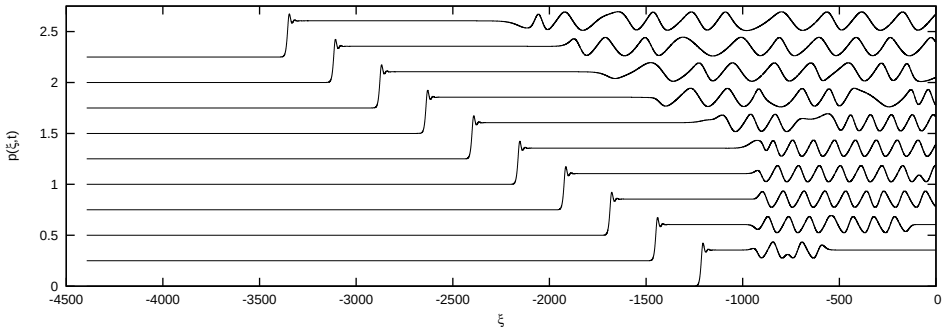

Fig. 2. Example of a transiently observed selected wave train. Shown are vertically spaced plots of the predator density at times (from bottom to top) t=1000, t=2000, ..., t=10000 for the model (iii) with parameters as in Table 1 and $\lambda_0 = 0.015$, $D_h = 1$, $D_p = 1$.

speed of the secondary transition. In all cases the speed of the wave train was computed as $c_{wtrain} = d/19 - c_{coh}$ where d is the distance travelled over the course of the 19 time units by the second peak of the wave train behind the primary invasion front. The distance d was numerically computed by a simple routine that tracked locations of local maxima chronologically through the set of profiles in the timeseries. These "observed" speeds for the various models are shown in comparison with the predicted speeds in Fig. 3.

We can see from the results shown in Fig. 3 that the performance of the criterion (16) is dependent on the particular model considered, as well as how far the parameter values are from the Hopf bifurcation in the kinetics. We first note that for the λ-ω model (i), the selection criterion developed in [13] and also here using the CGL equation performs extremely well, providing evidence that this selection mechanism is indeed valid at least for the λ-ω system. We can also observe from the data shown in Fig. 3 that for all three models (ii)-(iv) the criterion appears to provide a higher order prediction than the λ-ω system prediction near the Hopf bifurcation and so retains accuracy farther from it. For models (ii) and (iii), we eventually see the loss of accuracy for the pacemaker criterion as the parameter values are increased still farther from the

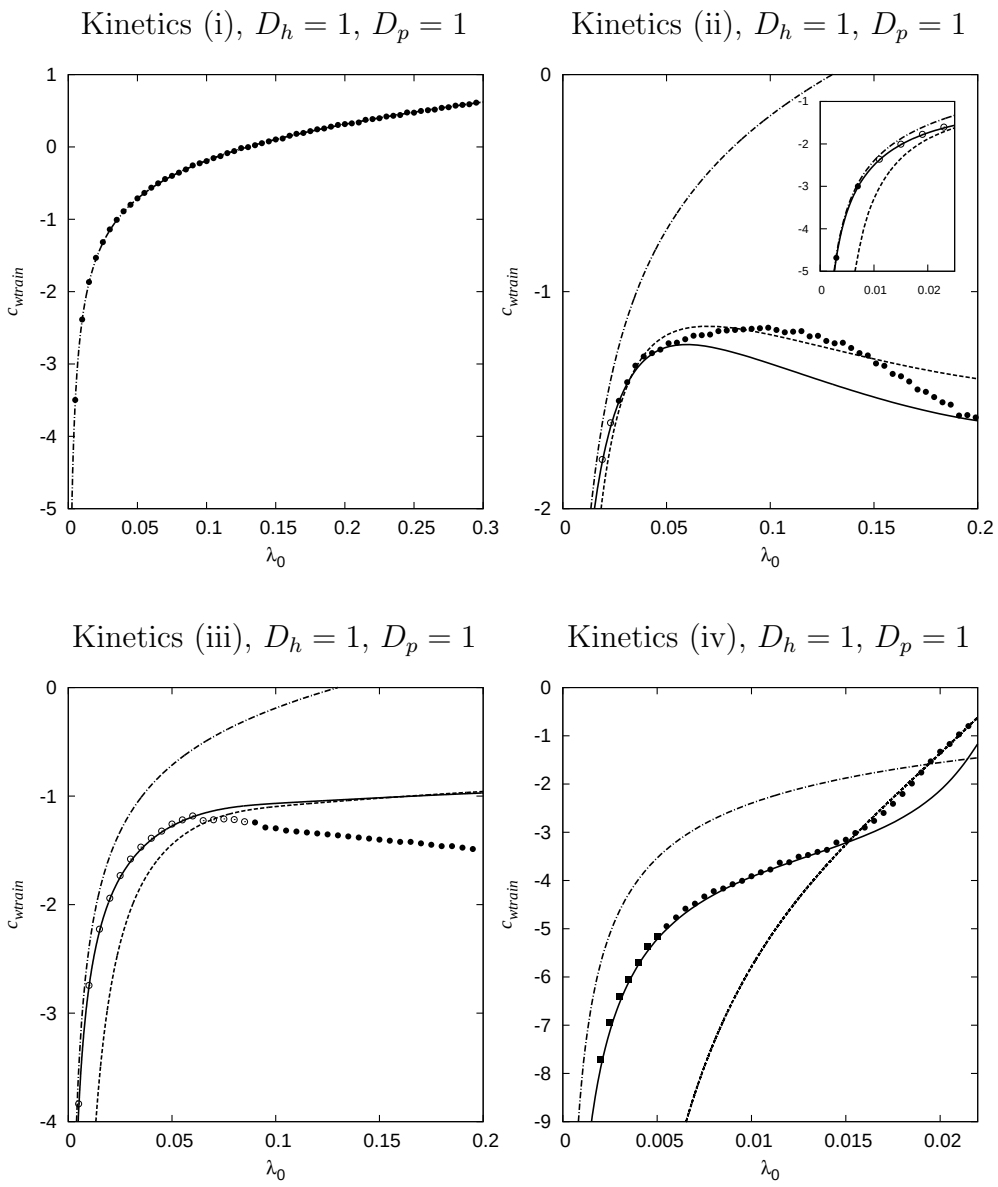

Fig. 3. Wave train speeds in numerical simulations compared with predictions for cases with equal diffusion coefficients. Horizontal axis is the bifurcation parameter λ_0. Vertical axis are the corresponding wave train speeds c_{wtrain}. Predictions using the λ-ω criterion (8) are dot-dashed lines. Predictions using the new pacemaker criterion (16) are solid lines for Case I (separated) and dashed lines for Case II (attached). Simulation observations are point symbols. Solid circles are speeds computed with final time $t = 10000$. Squares in the kinetics (iv) plot are speeds computed with final time $t = 20000$. Open circles are cases where the selected wave train was only observed transiently and speeds were then computed as described in the text. Inset of (ii) shows the region nearest the kinetic Hopf bifurcation.

bifurcation point. In the case of model (ii) this occurs after there is an apparent switch from Case I (separated) to Case II (attached) of the criterion whereas for model (iii) the observed speeds fall away from the prediction while still in the Case I region. In contrast, the pacemaker criterion performs extremely well for the entire parameter range chosen for model (iv).

5.2 Unequal Diffusion Coefficients

We also conducted a limited study for models (i) and (iv) with $D_h = 1$, $D_p = 0.5$ and models (ii) and (iii) with $D_h = 1$, $D_p = 2$. All other parameters were taken as in Table 1 and the procedure used is as described for equal diffusion coefficients above. In this case, initial solutions for the continuation of the selection criterion are obtained from the equal diffusion cases by first continuing to the appropriate value of the diffusion coefficient parameter D_p. With unequal diffusion coefficients the analytical prediction (8) breaks down, and so we illustrate that in this case the criterion (16) provides an improved prediction even for the kinetics (i). The results for the numerical simulations and the predicted speeds using (16) are shown in Fig. 4.

The results of this study for the case of unequal diffusion coefficients show that, at least for these examples, this criterion performs quite well even in the case of unequal diffusion coefficients. This suggests some promise for this criterion to apply to the more general and biologically relevant case of unequal predator and prey diffusion coefficients.

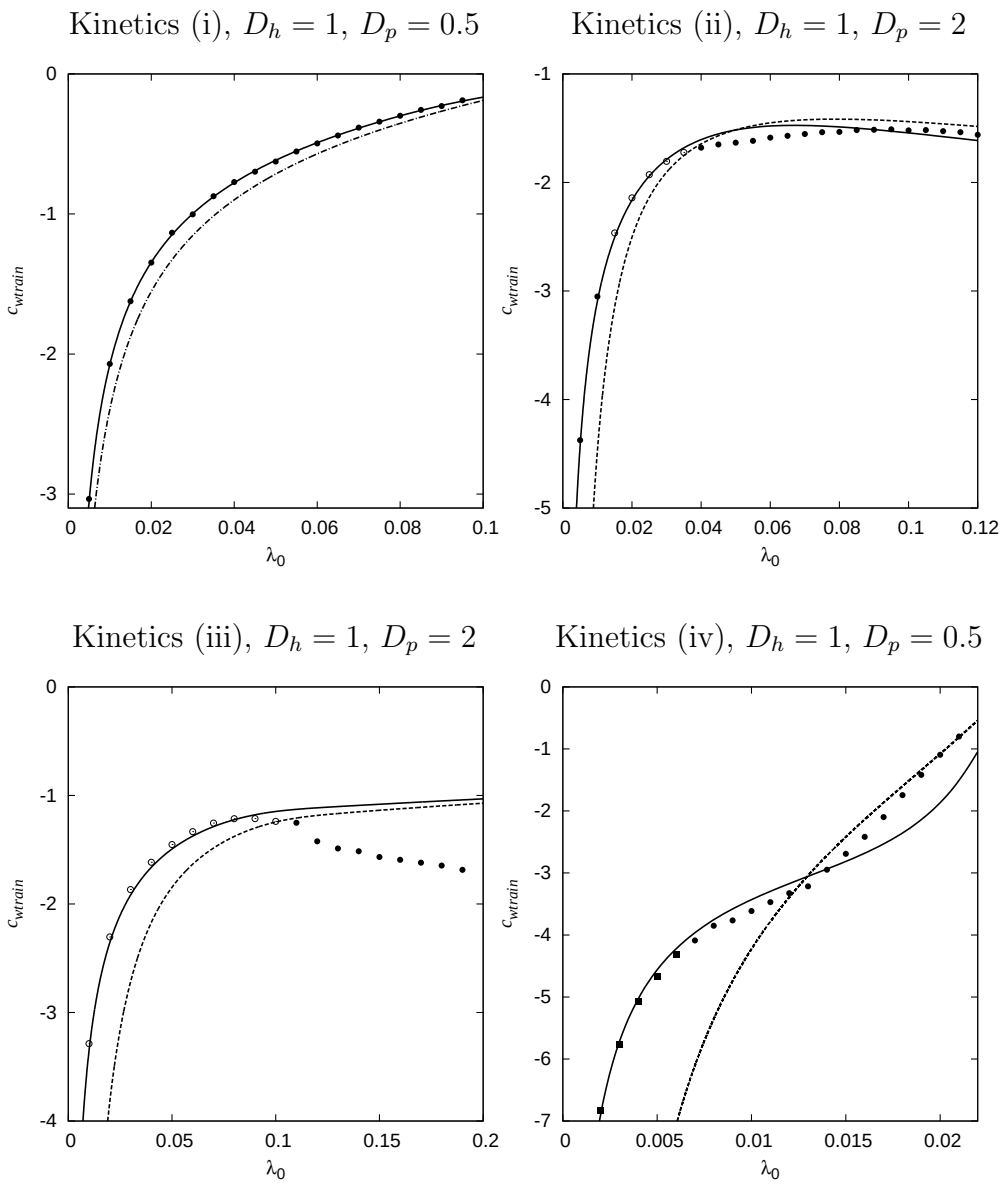

Fig. 4. Wave train speeds in numerical simulations compared with predictions for cases with unequal diffusion coefficients. Horizontal axis is the bifurcation parameter λ_0. Vertical axis are the corresponding wave train speeds c_{wtrain}. Curves and point symbols are as described for Fig. 3. For model (i), the analytical prediction (8) assuming $D_h = 1 = D_p$ is shown (dot-dashed curve) for comparison.

6 Discussion

The pacemaker criterion (16) developed here provides a relatively simple method for predicting the selection of wave trains following predator inva-

sions in oscillatory reaction-diffusion models. Our study of the performance of the pacemaker criterion for models (ii)-(iv) suggests that this criterion may in general give a good prediction for some range of parameters near the Hopf bifurcation in the kinetics. However, the performance of the pacemaker criterion is clearly model-dependent, and indeed since for each of the models chosen we studied only a small slice of parameter space it is possible that it would also be parameter-dependent. In fact, we have no *a priori* means of predicting when the pacemaker criterion will provide an accurate prediction. We can, however, identify a number of factors that may be responsible for deviation from the predictions of the pacemaker conjecture and suggest areas for future work.

Our development of the criterion assumes that there exists a front between a spatially homogeneous steady state (whether prey-only or coexistence) and the selected wave train. While visual inspection of numerical simulations suggests that such fronts do exist, we have no mathematical proof of this. Fronts of the type we assume to exist are called defects in [19]; they are solutions that are temporally periodic in some comoving frame and asymptotic in space to wave trains (or steady states). Defects are heteroclinic connections in an infinite-dimensional space of temporally periodic functions, and what is required is a proof that these heteroclinic connections indeed exist in the reaction-diffusion systems we consider. We also assume that this heteroclinic connection has the particular frequency ω_{coh}, given by the imaginary part of the eigenvalues of the linearization of the kinetics at the coexistence steady state. We chose this frequency because it extends the λ-ω system prediction and seems to perform well for the criterion. For Case I (separated) this is natural, and it is somewhat surprising that it can perform well even for Case II (attached) where the primary front does not approach the coexistence state.

Clearly, if our assumptions about the existence and frequency of the heteroclinic connection are false then we cannot expect the pacemaker criterion to be accurate. In fact, it is known that when there exist wave trains of the same speed c_{inv} as the primary invasion front the invasion may take place through a point-to-periodic heteroclinic connection in a single frame moving with speed c_{inv}, as studied by [29]. We performed a few numerical simulations in this parameter region for model (ii) with $D_h = 1$, $D_p = 2$ (beyond the parameter range shown in Fig. 4) and found that wave trains of speed c_{inv} appeared to be selected, rather than those predicted by the selection mechanism described here. One possible reason for the failure of our selection mechanism in this case is that for these parameter regions, which are far from the Hopf bifurcation in the kinetics, the heteroclinic connection we conjecture may not exist. We think it is therefore important to establish the existence of such heteroclinic connections for the full model under study, rather than just the λ-ω system. The coherent front solutions for the CGL equation are a special case of the more general "coherent pattern forming fronts" discussed in [14] and there may be a method to compute such coherent pattern forming fronts numerically by continuation in AUTO using the techniques described in [30] and references therein. While the numerical computation of these heteroclinic connections would not rigorously prove their existence, it would offer additional evidence for this proposed wave train selection mechanism and could open a path to further numerical work on the multiplicity and stability of such structures.

In this study we have made no reference to the stability of the wave trains and heteroclinic connections considered. In fact, in our simulations we observe two potential instabilities. The first is as shown in Fig. 2 where a front of (approximately) the predicted speed is only observed transiently. One possible reason for this transient behaviour is that the heteroclinic connection is unstable.

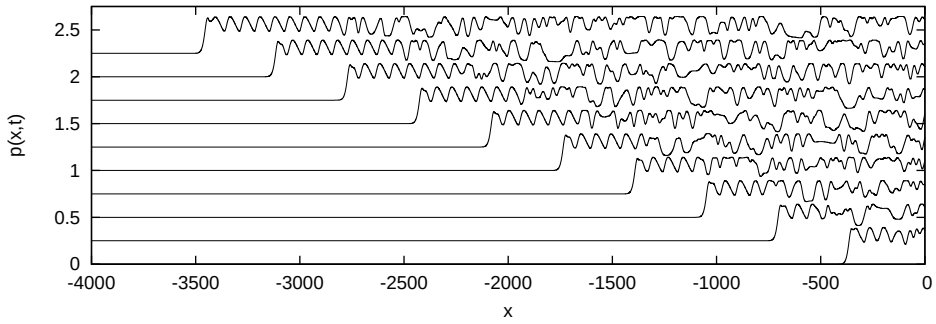

Fig. 5. Example of an unstable selected wave train. Shown are vertically spaced plots of the predator density in the stationary frame at times (from bottom to top) t=1000, t=2000, ..., t=10000 for the model (ii) with parameters as in Table 1 and $\lambda_0 = 0.04$, $D_h = 1$, $D_p = 1$.

Since our numerical simulations are for finite times, it is in fact possible that even the simulations that remained regular (closed circles in Figs. 3 and 4) are transients. The study of the stability of the heteroclinic connections assumed by the selection criterion would therefore be an important area of future study.

A second form of instability that we see in our simulations is shown in Fig. 5. This figure is shown in the stationary frame for illustration. In this case, a selected wave train is observed behind the initial predator invasion front, but becomes irregular further back, a solution form that has been noted for predator invasions in a number of studies and attributed to the instability of the wave train [8,31]. The physics literature has long noted that wave trains may be either convectively or absolutely unstable [32]. When a solution is convectively unstable in a given frame of reference, localized perturbations will grow, but will be convected away quickly enough that at a fixed position in the frame of reference the perturbation in fact decays. If the solution is absolutely unstable in the frame of reference, however, perturbations grow at any fixed position. In our simulations in the comoving frame c_{coh}, irregularities such as those shown in Fig. 5 were convected away through the boundary and so these selected wave trains are presumably only convectively unstable. It

would be interesting to determine whether this is generally the case or whether absolutely unstable wave trains may also be selected. We expect that methods developed in [33] would be useful to numerically study this problem, and these have recently been applied by Sherratt et al (2009) to wave train solutions of λ-ω systems [31]. For the other predator-prey models studied here we have used these methods to compute the essential spectra of wave trains for a few cases and found the selected wave trains to be unstable. However, we have been unable to compute the absolute spectra of non-sinusoidal wave trains and so the nature of instabilities of selected wave trains in general remains an open problem.

Finally, as we saw in our study of models with unequal predator and prey diffusion coefficients the developed criterion appears to be useful for prediction of wave train selection when the predator and prey species do not diffuse with the same strength. Since in natural systems species likely have different movement rates, this would be a substantial advance. However, we have only shown here a few cases and so the application of the criterion to unequal diffusion coefficients in general requires further study. Here again rigourous mathematical work on the existence of the assumed heteroclinic connections should be useful.

Acknowledgements

This work was partially supported by funding from the Natural Sciences and Engineering Research Council of Canada (NSERC). As well, S.M. would like to acknowledge the Pacific Institute for the Mathematical Sciences (PIMS) for funding through the IGTC fellowship program. We would also like to thank

Michael Doebeli and his lab group for many helpful comments and suggestions. Finally, we are grateful for the comments and suggestions of two anonymous referees as we think they helped greatly improve the manuscript.

A Linear Spreading Speeds

In this appendix we describe how to compute the linear spreading speeds using (3) for the oscillatory reaction-diffusion system (1). We assume the exponential ansatz $h, p \sim e^{i(kx-\omega t)}$ for perturbations of the linearized system. This gives the characteristic equation with

$$\begin{aligned} S(k,\omega) = &-\omega^2 + i\omega\left[-k^2(D_h + D_p) + a_{1,1} + a_{2,2}\right] + D_h D_p k^4 \\ &-D_p a_{1,1} k^2 - D_h a_{2,2} k^2 + a_{1,1}a_{2,2} - a_{1,2}a_{2,1} \end{aligned} \tag{A.1}$$

where

$$a = \left[\begin{array}{cc} \frac{\partial f}{\partial h} & \frac{\partial f}{\partial p} \\ \\ \frac{\partial g}{\partial h} & \frac{\partial g}{\partial p} \end{array}\right]_{(h_0,p_0)}$$

is the linearization matrix about the steady state (h_0, p_0). Therefore, for the system (1) the linear spreading speed equations (3) are (dropping the stars)

$$\begin{aligned} 0 = &-\omega^2 + i\omega\left[-(D_h + D_p)k^2 + a_{1,1} + a_{2,2}\right] + D_h D_p k^4 - D_p a_{1,1} k^2 \\ &-D_h a_{2,2} k^2 + a_{1,1}a_{2,2} - a_{1,2}a_{2,1} \end{aligned} \tag{A.2}$$

$$\begin{aligned} 0 = &-2i\omega(D_h + D_p)k + 4D_h D_p k^3 - 2D_h a_{2,2} k - 2D_p a_{1,1} k - 2\nu\omega \\ &-i\nu(D_h + D_p)k^2 + i\nu(a_{1,1} + a_{2,2}) \end{aligned} \tag{A.3}$$

$$0 = \Im(\omega - \nu k) \tag{A.4}$$

Typically, for given values of a, D_h and D_p the system of equations (A.2)-(A.4) and hence the linear spreading speed ν^* must be solved for numerically. Indeed, for our use in this study we numerically continued solutions of (A.2)-(A.4) as 5 real equations in tandem with the wave train selection criterion. In addition, we track the quantity

$$D = \frac{-\omega(D_h + D_p) - 6iD_hD_pk^2 + iD_ha_{2,2} + iD_pa_{1,1} - 2\nu(D_h + D_p)k + i\nu^2}{-2\omega - i(D_h + D_p)k^2 + ia_{1,1} + ia_{2,2}}$$

to ensure that we are at a dynamically relevant saddle point. For the special case $D_h = D_p = 1$ considered for models (i)-(iv) in this study, we can solve for the linear spreading speeds c_{inv} and c_{sec} analytically, as we show in the following section. We use these analytical results as the initial solution for the continuation of (A.2)-(A.4). For the unequal diffusion cases in this study we begin from the analytical prediction for $D_h = D_p = 1$ and first continue in the diffusion coefficient D_p.

A.1 Linear Spreading Speeds for the Equal Diffusion Cases

When $D_h = D_p = 1$ we have from (A.3) that either $\nu = -2ik$ or $\omega = -ik^2 + i(a_{1,1} + a_{2,2})/2$. The second case is in general inconsistent with (A.2) and so we assume the first case, ie. that $\nu = -2ik$. In this case, k must be purely imaginary and taking $k = i\gamma,\ \gamma \in \mathbb{R}$ in (A.4) gives $\Im(\omega) = 2\gamma^2$. Hence, we take $\omega = \alpha + 2i\gamma^2$, $\alpha \in \mathbb{R}$ in (A.2) and get the following two real equations for α and γ.

$$\begin{aligned} 0 &= \gamma^4 + \gamma^2(-a_{1,1} - a_{2,2}) - \alpha^2 + a_{1,1}a_{2,2} - a_{1,2}a_{2,1} \\ 0 &= \alpha(2\gamma^2 - a_{1,1} - a_{2,2}). \end{aligned} \tag{A.5}$$

Computing c_{sec} for $D_h = D_p = 1$:

This is the speed obtained by linearizing about the spatially homogeneous coexistence steady state $(h_0, p_0) = (h^*, p^*)$. The second equation in (A.5) has the possible solution $\alpha = 0$. In this case, solution of the first equation for γ using $\alpha = 0$ yields

$$\gamma^2 = \frac{a_{1,1} + a_{2,2}}{2} \pm \frac{1}{2}\sqrt{(a_{1,1} - a_{2,2})^2 + 4a_{1,2}a_{2,1}}.$$

We assume for the selection criterion that ω_{coh} as defined in (17) is real and so the expression on the right has non-zero imaginary part. We therefore assume $\alpha \neq 0$ and so from the second equation of (A.5) we have $\gamma^2 = (a_{1,1} + a_{2,2})/2$. Then using $\nu^* = 2\gamma$ we have the linear spreading speed

$$c_{sec} = \sqrt{2(a_{1,1} + a_{2,2})}$$

for rightward moving fronts emanating from the coexistence steady state.

Computing c_{inv} for $D_h = D_p = 1$:

This is the linear spreading speed for fronts emanating from the spatially homogeneous prey-only steady state $(h_0, p_0) = (1, 0)$. In this case, for models (ii)-(iv) we have $a_{1,1} < 0$, $a_{1,2} < 0$, $a_{2,1} = 0$ and $a_{2,2} > 0$. Therefore, if $\alpha \neq 0$ the first equation of (A.5) gives

$$\alpha^2 = -\frac{1}{4}(a_{1,1} + a_{2,2})^2 + a_{1,1}a_{2,2}$$

which contradicts α being real. We therefore take $\alpha = 0$ and solve to get $\gamma^2 = a_{2,2}$. We thus have the linear spreading speed

$$c_{inv} = 2\sqrt{a_{2,2}}$$

for rightward moving fronts emanating from the prey-only steady state.

References

[1] J. D. Murray, Mathematical Biology I: An Introduction, 3rd Edition, Springer-Verlag, 2002.

[2] O. N. Bjørnstad, M. Peltonen, A. M. Liebhold, W. Baltensweiler, Waves of larch budmoth outbreaks in the European Alps, Science 298 (2002) 1020–1023.

[3] X. Lambin, D. A. Elston, S. J. Petty, J. L. MacKinnon, Spatial asynchrony and periodic travelling waves in cyclic populations of field voles, Proc. R. Soc. Lond., Ser. B: Biol. Sci. 265 (1998) 1491–1496.

[4] J. L. MacKinnon, S. J. Petty, D. A. Elston, C. J. Thomas, T. N. Sherratt, X. Lambin, Scale invariant spatio-temporal patterns of field vole density, Ecology 70 (2001) 101–111.

[5] R. Moss, D. A. Elston, A. Watson, Spatial asynchrony and demographic traveling waves during red grouse population cycles, Ecology 81 (2000) 981–989.

[6] E. Ranta, V. Kaitala, Travelling waves in vole population dynamics, Nature 390 (1997) 456.

[7] E. Ranta, V. Kaitala, J. Lindstrom, Dynamics of Canadian lynx populations in space and time, Ecography 20 (1997) 454–460.

[8] J. A. Sherratt, M. J. Smith, Periodic travelling waves in cyclic populations: field studies and reaction-diffusion models, J. R. Soc. Interface 5 (2008) 483–505.

[9] J. A. Sherratt, B. T. Eagan, M. A. Lewis, Oscillations and chaos behind predator-prey invasion: mathematical artifact or ecological reality?, Phil. Trans. Roy. Soc. Lond. B 352 (1997) 21–38.

[10] J. A. Sherratt, M. A. Lewis, A. C. Fowler, Ecological chaos in the wake of invasion, Proc. Natl. Acad. Sci. 92 (1995) 2524–2528.

[11] M. J. Smith, J. A. Sherratt, The effects of unequal diffusion coefficients on periodic travelling waves in oscillatory reaction-diffusion systems, Physica D 236 (2007) 90–103.

[12] N. Kopell, L. N. Howard, Plane wave solutions to reaction-diffusion equations, Stud. Appl. Math. 52 (1973) 291–328.

[13] J. A. Sherratt, Invading wave fronts and their oscillatory wakes are linked by a modulated travelling phase resetting wave, Physica D 117 (1998) 145–166.

[14] W. van Saarloos, Front propagation into unstable states, Phys. Rep. 386 (2003) 29–222.

[15] I. S. Aranson, L. Kramer, The world of the complex Ginzburg-Landau equation, Rev. Mod. Phys. 74 (2002) 99–143.

[16] M. van Hecke, Coherent and incoherent structures in systems described by the 1D CGLE: experiments and identification, Physica D 174 (2003) 134–151.

[17] M. van Hecke, C. Storm, W. van Saarlos, Sources, sinks and wavenumber selection in coupled CGL equations and experimental implications for counter-propagating wave systems, Physica D 134 (1999) 1–47.

[18] W. van Saarloos, P. C. Hohenberg, Fronts, pulses, sources and sinks in generalized complex Ginzburg-Landau equations, Physica D 56 (1992) 303–367.

[19] B. Sandstede, A. Scheel, Defects in oscillatory media: toward a classification, SIAM J. Appl. Dyn. Syst. 3 (2004) 1–68.

[20] U. Ebert, W. van Saarloos, Front propagation into unstable states: universal algebraic convergence towards uniformly translating pulled fronts, Physica D 146 (2000) 1–99.

[21] S. V. Petrovskii, H. Malchow, Wave of chaos: new mechanism of pattern formation in spatio-temporal population dynamics, Theor. Popul. Biol. 59 (2001) 157–174.

[22] J. Huang, G. Lu, S. Ruan, Existence of traveling wave solutions in a diffusive predator-prey model, J. Math. Biol. 46 (2003) 132–152.

[23] J. D. M. Rademacher, A. Scheel, Instabilities of wave trains and turing patterns, Int. J. Bif. Chaos 17 (2007) 2679–2691.

[24] J. A. Sherratt, Periodic travelling waves in cyclic predator-prey systems, Ecol. Lett. 4 (2001) 30–37.

[25] Y. A. Kuznetsov, Elements of Applied Bifurcation Theory, Vol. 112 of Applied Mathematical Sciences, Springer-Verlag, 1995.

[26] E. J. Doedel, A. R. Champneys, T. F. Fairgrieve, Y. A. Kuznetsov, B. Sandstede, X. Wang, AUTO97: Continuation and Bifurcation Software for Ordinary Differential Equations (with HomCont), Concordia University (1997).

[27] M. J. Friedman, E. J. Doedel, Numerical computation and continuation of invariant manifolds connecting fixed points, SIAM J. Numer. Anal. 28 (1991) 789–808.

[28] B. Krauskopf, H. M. Osinga, E. J. Doedel, M. E. Henderson, J. Guckenheimer, A. Vladimirsky, M. Dellnitz, O. Junge, A survey of methods for computing (un)stable manifolds of vector fields, Int. J. Bifurcat. Chaos Appl. Sci. Eng. 15 (2005) 763–791.

[29] S. R. Dunbar, Traveling waves in diffusive predator-prey equations: periodic orbits and point-to-periodic heteroclinic orbits, SIAM J. Appl. Math. 46 (1986) 1057–1078.

[30] A. R. Champneys, B. Sandstede, Numerical computation of coherent structures, in: B. Krauskopf, H. M. Osinga, J. Galan-Vioque (Eds.), Numerical Continuation Methods for Dynamical Systems, Springer, 2007, pp. 331–358.

[31] J. A. Sherratt, M. J. Smith, J. D. M. Rademacher, Locating the transition from periodic oscillations to spatiotemporal chaos in the wake of invasion, Proc. Natl. Acad. Sci. 106 (2009) 10890–10895.

[32] R. J. Briggs, Electron-stream interaction with plasmas, MIT Press, 1964.

[33] J. D. M. Rademacher, B. Sandstede, A. Scheel, Computing absolute and essential spectra using continuation, Physica D 229 (2007) 166–183.